IEEE Photonics Journal
An IEEE Photonics Society Publication

Open Access

Analysis of Lasing in Dye-Doped Photonic Crystals

Volume 5, Number 1, February 2013

M. Srinivas Reddy
Sunita Kedia
Ramarao Vijaya
Alok Kumar Ray
Sucharita Sinha
Ivan D. Rukhlenko
Malin Premaratne, Senior Member, IEEE

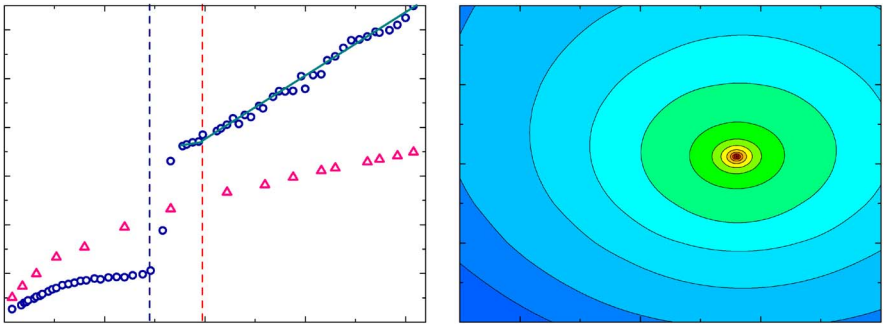

DOI: 10.1109/JPHOT.2013.2241754
1943-0655/$31.00 ©2013 IEEE

Analysis of Lasing in Dye-Doped Photonic Crystals

M. Srinivas Reddy,[1,2,3] Sunita Kedia,[2,4] Ramarao Vijaya,[5] Alok Kumar Ray,[6] Sucharita Sinha,[6] Ivan D. Rukhlenko,[3] and Malin Premaratne,[3] *Senior Member, IEEE*

[1]IITB-Monash Research Academy, CSE Building 2nd Floor, IIT Bombay, Powai, Mumbai 400076, India
[2]Department of Physics, Indian Institute of Technology Bombay, Powai, Mumbai 400076, India
[3]Advanced Computing and Simulation Laboratory (AχL), Department of Electrical, Computer Systems Engineering, Monash University, Clayton, Victoria 3800, Australia
[4]Theoretical Physics Division, Physical Research Laboratory, Ahmedabad 380009, India
[5]Department of Physics, Indian Institute of Technology Kanpur, Kanpur 208016, India
[6]Laser and Plasma Technology Division, Bhabha Atomic Research Centre, Mumbai 400085, India

DOI: 10.1109/JPHOT.2013.2241754
1943-0655/$31.00 ©2013 IEEE

Manuscript received December 5, 2012; revised January 15, 2013; accepted January 16, 2013. Date of publication January 22, 2013; date of current version February 4, 2013. This work was supported by the Board of Research in Nuclear Sciences, India. The works of I. D. Rukhlenko and M. Premaratne were supported by the Australian Research Council through its Discovery Early Career Researcher Award DE120100055 and Discovery Grant DP110100713, respectively. Corresponding author: I. D. Rukhlenko (e-mail: ivan.rukhlenko@monash.edu).

Abstract: Recently, we experimentally demonstrated room-temperature lasing of self-assembled opal photonic crystal (PhC) made of rhodamine-B-doped polystyrene colloids. Here, we explain this experimental observations by analyzing the phenomenon of light amplification in dye-activated PhCs via a complex-valued permittivity of the colloids. We show that the lasing is facilitated by the enhanced distributed feedback due to the reduced group velocity in the vicinity of the photonic band edge. This simple approach to the analysis of PhC lasing behavior allows us to calculate the lasing wavelength in close agreement with the experimental value. It also enables the estimation of gain coefficient required for lasing and may prove useful in design of compact PhC-based lasers.

Index Terms: Photonic crystals (PhCs), photonic crystal lasers, dye lasers.

1. Introduction

Photonic crystals (PhCs) are artificial structures containing a periodically varying refractive index, with a periodicity in the order of the optical wavelength. They have found many applications in the areas of optoelectronics and communication devices, due to their ability to control, manipulate, and localize light [1]–[3]. The periodicity of PhCs results in dispersion diagrams containing a series of allowed and forbidden bands. As a result of this, the propagation of light is prohibited either in certain directions (resulting in a pseudophotonic stopband) or in all directions (providing a complete stopband), depending on the periodicity, index contrast, and crystal structure. The density of electromagnetic modes at a given frequency—the local density of states (LDOS)—is reduced inside the photonic band gap and increased near the band edges. With an active medium present inside a PhC, it is possible to tune the emission characteristics of the active medium cleverly in certain frequency ranges depending on the extent of overlap of the emission band with the photonic stopband [4]–[8].

Enhancement of emission from a PhC can be achieved either through localization of light, which minimizes the mode volume at a defect serving as an ultrasmall high-quality microcavity [3], or by reducing the group velocity near the band edges exploiting enhanced distributed feedback (DFB) thus increasing the interaction time between the light and gain medium [9]. This has been realized and demonstrated via enormous theoretical and experimental efforts towards attaining lasing from two-dimensional PhC with either defect [10]–[13] or enhanced DFB modes [14]–[16]. Moreover, a few works in the literature also experimentally demonstrate lasing phenomenon from active 3-D opaline structures [17]–[20].

To the best of our knowledge, no experimental work supported with theory has been done to quantify the effect of lasing in dye-activated opal PhCs. However, such a combined study is in high demand, since it would allow one to explain the effect of photonic band structure on the emission characteristics and to exclude other mechanisms such as nonlinear effects. It will also give a boost to application-oriented research. In an earlier work [21], some of us had reported room-temperature lasing from a large, all-solid sample of self-assembled PhC, which took only 3 h to fabricate. Each polystyrene colloid in the PhC was doped with rhodamine-B (RhB), thus avoiding the need of infiltration of the gain medium after the growth of the PhC and resulting in its uniform distribution throughout the PhC. In view of the overlap of the emission band of RhB with the stopband of the PhC, the lasing is facilitated by large DFB, enhanced due to the small group velocity of the propagating modes, and occurs in the visible region near the photonic band edge. We measured the emission spectra of the fabricated PhC for different pump powers. The amplified spontaneous emission (ASE) was observed at about 70 mW of pump power and lasing at a high-frequency edge of the stopband, with a lasing threshold of about 99 mW. In this work, we calculate the lasing wavelength using the Korringa–Kohn–Rostoker (KKR) method by an extremely simple and intuitive approach of using a negative valued imaginary part in the permittivity of the colloids. The calculated value of the lasing wavelength is found to be in close agreement with the experimentally obtained value. We also estimate the threshold gain coefficient, which will help to design compact PhC lasers.

The paper is organized as follows: In Section II, we provide the basic information about the preparation of the sample and the experimental setup used to study its emission properties. The laser-induced emission from the PhC is studied in Section III, while Section IV presents the results of numerical simulations. We summarize our results and conclude the paper in Section V.

2. Sample Fabrication and Experimental Details

The PhCs were fabricated using the commercially available RhB-doped polystyrene (PS-RhB) colloidal suspensions from M/s Microparticles GmbH, with a mean colloidal diameter of 302 nm. The diameter was chosen so that the intrinsic emission from the dye overlaps with the photonic stopband along the ΓL direction. The inward-growing self-assembly method discussed in [22] was used to synthesize the PhCs. The samples were grown on a clean glass substrate (with an area of 2.5×2.5 cm^2) in a time span of 3 h. The structural quality of the fabricated PhCs was investigated using the field-emission-gun scanning electron microscopy (FEGSEM). The FEGSEM images revealed the grain structure of the PhCs, with well-ordered domains separated by cracks. This structure occurs due to a slight shrinkage of the sample during its annealing and cannot be avoided in PhCs fabricated using self-assembly methods. Reflection measurements were carried out using Perkin Elmer Lambda 950 spectrophotometer with a universal reflectance accessory. The halogen lamp was used as the source of the unpolarized light (with a beam cross section area of 5×5 mm^2) in the measurements.

Frequency-doubled Nd:YAG laser (repetition rate, 10 Hz; pulsewidth, $\sim$6 ns) operating at 532 nm was used as a pump, to excite the dye-doped PhCs in the laser-induced emission studies. The laser beam was incident on the PhC after passing through a plano-convex lens with a focal length of 10 cm; the lens was placed at a distance of 9 cm from the surface of the PhC. The excitation was kept normal to the surface, and the emission was collected at different angles from the normal to the surface. More details are reported in [21].

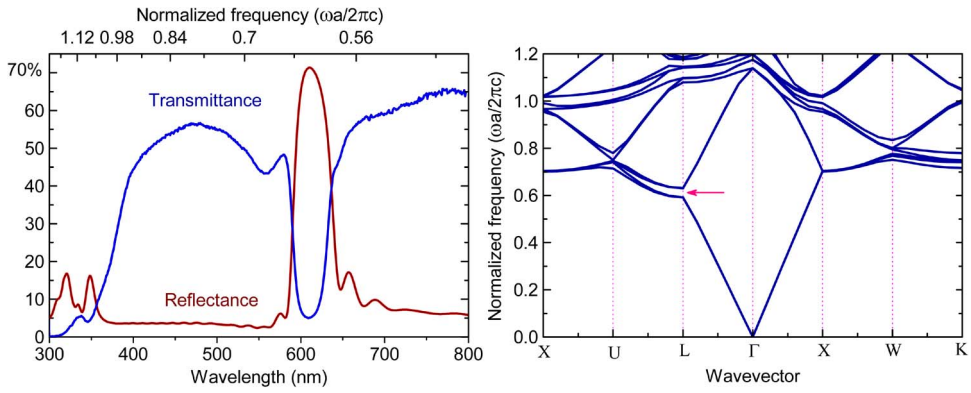

Fig. 1. (a) Experimental reflection and transmission spectra from the (111) plane of PhC made of PS-RhB nanospheres with a diameter of 302 nm. (b) Band structure of PS-RhB PhC calculated using the plane-wave expansion method. Position of the *L* gap is indicated by the horizontal arrow. The best agreement between the theoretical and experimental stopbands is achieved for nanosphere diameter of 268 nm.

3. Experimental Results and Discussion

3.1. Reflection Measurements

The reflectance and transmittance spectra measured from the (111) plane of the PS-RhB PhC are shown in Fig. 1(a). The signature of the photonic stopband is clearly seen as a reflection peak, with its corresponding trough in the transmission. The reflectance was measured at 8° from the normal incidence, while the transmittance was measured at normal incidence. The 71% reflectance peak located at about 611 nm is supplemented by a trough in the transmission spectra with a transmittance of about 5%. It is ascribed to the photonic stopband in the [111] direction of a fcc structure, as it is evident by comparing the normalized frequency units shown at the top of Fig. 1(a) with the band diagram in Fig. 1(b). The band diagram was calculated in the plane-wave basis using block-iterative frequency-domain method [23]. The reflection peak in the experimental spectrum is slightly shifted towards the shorter wavelengths with respect to the stopband center but agrees well with the theoretical prediction when a diameter of 268 nm is assumed for spheres constituting the PhC (this diameter is used in the calculations throughout the rest of the paper). The asymmetry in shapes of the reflection and transmission spectra is due to the domain cracks in the crystalline structure of the PhC. Due to light scattering at these cracks, they also lead to the broadening and flattening of the spectral features [24]. The effect of the PhC defects was unavoidable in the reflection measurements, since the PhC area illuminated in the experiments (several millimeters in diameter) was much larger than the average size of the domain crack (about 60–70 μm).

The photonic strength (Ψ) of the reflection peak is seen to be 6.7%, which is close to the value of 6.5% calculated from the band diagram. The Bragg length defined by $l_{\text{Bragg}} = 2d_{hkl}/(\pi\Psi)$, which is the characteristic distance that light can propagate along the [hkl] direction inside a PhC with the interplanar distance of d_{hkl} [25], was estimated to be 2.3 μm for $d_{111} \approx 247$ nm. The Fabry–Perot (FP) oscillations around the reflection spectrum are the clear evidence of the periodic arrangement of the PhC layers. The thickness t of the PhC was found to be 7.1 μm, based on the features of the FP fringes [26]. It is of significance that $t \gg l_{\text{Bragg}}$ and, hence, our sample was immune to finite-size effects [27]. The higher-order stopgaps at the lower-wavelength sides of the small reflection peaks (located around 300–360 nm) serve as another indication of the superior quality of the synthesized PhCs [28].

3.2. Emission Measurements

The measured angle-dependent reflection spectra (not shown here) span over the wavelength range from 557 to 611 nm for the incident angles between 40° and 8° from the surface normal (ΓL direction). As the emission from the RhB occurs in the same wavelength range, a strong

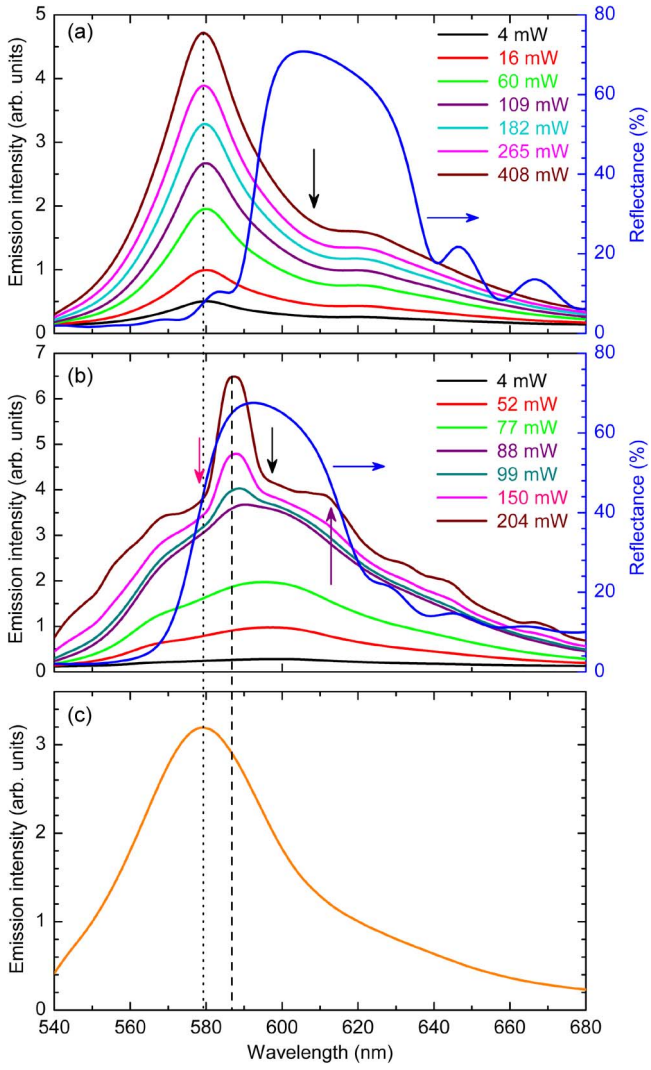

Fig. 2. Emission spectra of PS-RhB PhC measured for (a) $L + 10^\circ$ and (b) $L + 22^\circ$ collection directions and different pump powers. Blue are the corresponding reflection spectra. (c) Reference photoluminescence spectra of PS-RhB PhC measured for $L + 60^\circ$ collection direction, when the impact of the band gap on the emission is absent.

modification of the emission from PS-RhB PhC can be expected in this angular range. Our recent study [29] of the all-angle-dependent emission from similar PhCs (but of a slightly different colloidal diameter) confirms this expectation.

The emission spectra of the PS-RhB PhC for a wide range of pump powers are shown in Fig. 2. Fig. 2(a) and (b) correspond to the situations where emission was collected along the $L + 10^\circ$ and $L + 22^\circ$ directions (the $L + X^\circ$ direction is the direction that makes an angle X° with the normal to the surface of the PhC). For reference, the respective photonic stopbands, measured with an external light source, are shown by blue curves. The effect of the stopgap in both cases is clearly seen as a suppression in emission, which is independent of pump power, marked by the black vertical arrows. It is also seen that the change in the measurement direction from $L + 10^\circ$ to $L + 22^\circ$ results in blue shift of the trough in the emission spectra and photonic stopband, in full agreement with the Bragg law. As the position of the stopband at $L + 60^\circ$ does not overlap with the photoluminescence spectrum of RhB, the emission from RhB measured in this direction is considered to be intrinsic and taken as a reference in the further analysis of the stopband effect on

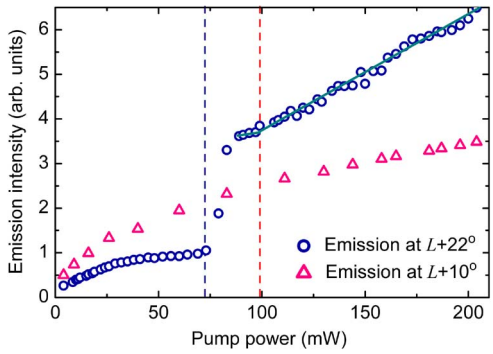

Fig. 3. Peak emission intensity at 587 nm (open circles) versus pump power collected at $L + 22^{\circ}$ direction illustrating the onset of lasing from PS-RhB PhC. Lasing threshold of 99 mW is shown by right dashed line. An abrupt increase in the emission intensity above 70 mW (left dashed line) is attributed to ASE. The measured peak emission intensity as a function of pump power in $L + 10^{\circ}$ direction for 580 nm (open triangles) shows monotonous increase with pump power. The experimental settings are the same as in Fig. 2.

emission [29]. The reference photoluminescence spectrum collected at $L + 60^{\circ}$ is shown in Fig. 2(c).

Fig. 2(a) shows that the increase in pump power to as high values as 400 mW does not significantly change the shape of the emission spectra near the peak wavelength (580 nm) of the reference spectrum, which is due to the fact that this wavelength (marked by the dotted vertical line) is relatively far from the edge of the photonic stopband. On the other hand, the close proximity of the photoluminescence peak and the photonic stopband for the collection direction of $L + 22^{\circ}$ in Fig. 2(b) results in dramatic reshaping of the emission from the PS-RhB PhC at high pump powers. At low pump powers, a broad emission spectrum [with a full width at half-maximum (FWHM) of 65 nm] centered at 598 nm is observed.

It can be also observed from Fig. 2(b) that the increase in the pump power up to 99 mW does not significantly change the emission spectrum. However, a prominent emission peak (with FWHM of about 9 nm) starts forming at this power near the low-wavelength edge of the photonic stopband, around 587 nm (marked by the dashed vertical line). The intensity of the peak grows steeply along with gain narrowing with increase of pump power, indicating the onset of lasing. It is well known that, in opal PhCs irrelevant to the spectral position of the stopband, random lasing always takes place at the peak wavelength of the photoluminescence band [30]. Since the lasing wavelength in our case does not coincide with the photoluminescence peak wavelength of 580 nm, the observed peak cannot be explained by the effect of random lasing. It is also found that variations in pump power do not influence the position and FWHM of the peak, which implies that optical nonlinearities (either in RhB or in polystyrene) are insignificant in emission process [17]. The experiments performed in several regions of the sample lead to the same conclusion. The sharp peak in the emission spectrum of PS-RhB PhC can be attributed to the photonic band edge lasing, which is facilitated by the DFB enhancement due to the reduced group velocity at the low-wavelength edge of the stopband. A detailed analysis of the DFB lasing mechanism will be given in Section IV.

Once the lasing threshold is reached, a clear trough (marked by the vertical pink arrow) appears on the blue side of the lasing peak [see Fig. 2(b)]. The trough is explained by the conversion of the spontaneous emission into stimulated emission, due to the feedback provided by Bragg planes of the PhC. Besides the main emission peak, a small enhancement of the spontaneous emission is observed near the long-wavelength edge of the stopband (the corresponding peak is marked by the vertical purple arrow). The enhancement is a result of the increase in LDOS in the vicinity of the band edge.

Fig. 3 shows (open circles) how the intensity of emission from PS-RhB PhC, measured at the wavelength of 587 nm and collected from the $L + 22^{\circ}$ direction [see Fig. 2(b)], varies with the pump power. The experimental data is seen to belong to three different regions. The first region below

70 mW represents the spontaneous emission from the PhC. The second region (from 70 to 99 mW) is characterized by the abrupt three-fold rise in the emission intensity. The rise is a manifestation of ASE, which occurs due to the increase in LDOS near the band edge. The stimulated emission from PS-RhB PhC takes place in the last region, where pump power exceeds the photonic-band-edge lasing threshold of 99 mW. The abrupt change (at 99 mW) in the slope of the linear fit (solid light-blue curve) to the experimental data is a clear manifestation of the threshold effect. This region is characterized by the formation of a narrow emission peak in Fig. 2(b). In comparison, the emission intensity of peak wavelength (580 nm) measured from the $L + 10^{\circ}$ direction (open triangles) shows a monotonous increase with pump power.

4. Numerical Results and Discussion

Since RhB providing optical gain is distributed uniformly inside each colloid of the PhC, the influence of the photonic stopband on emission can be modeled by allowing for gain through the complex-valued permittivity $\varepsilon = \varepsilon' + i\varepsilon''$ $(\varepsilon'' < 0)$ of polystyrene [31]. In the vicinity of the PhC band edges, the photon dispersion is nearly flat, and the group velocity is significantly reduced compared with its values inside the band. The enhancement in the emission efficiency near the band edge can be explained as a consequence of the respective increase in the interaction time between the RhB atoms and the radiation field. If the group velocity of the propagating mode is much smaller than the speed of light in a vacuum, then the lasing threshold $\varepsilon''_{\text{th}}$ (which is a measure of population inversion) is proportional to the square of the group velocity [31]. The smaller the group velocity is, the lower the lasing threshold.

We calculate the lasing wavelength and lasing threshold for PS-RhB PhC using the KKR method [32], [33]. Our numerical routine closely follows that developed for DFB lasers [34], by assuming that the population inversion of the uniformly doped RhB dye is achieved by means of optical pumping and that the system is ready to emit. Since it is a process of light emission without input signal, which is similar to the oscillations in electric circuits, the onset of lasing is equivalent to the divergence of either reflectance or transmittance, or sum of the reflectance and transmittance of the system [31]. Therefore, we calculate the reflectance spectrum of PS-RhB PhC as a function of ε'' and attribute its divergency to the lasing conditions. The energy loss due to both the spontaneous emission and PhC defects is neglected in our paper, without significantly affecting the lasing wavelength.

The reflection spectrum of PS-RhB PhC is calculated using 41 reciprocal two-dimensional wave vectors in the plane-wave expansion and spherical waves with angular momenta $l = 1, 2, \ldots, 7$, to get the converging results with the KKR method. For these calculations, the real part of the permittivity of polystyrene is taken to be $\varepsilon' = 2.5281$ and 28 number of layers [obtained from the FP fringes of reflection spectrum shown in Fig. 1(a)] were used. The accuracy with which our numerical simulations predict the PhC stopband may be estimated from Fig. 4, by comparing the band diagram with the reflection spectra calculated for $\varepsilon'' = 0$ and $\varepsilon'' = -0.02$, -0.04, and -0.05.

From Fig. 4(a), it can be observed that there is a photonic stopband in the normalized-frequency range of 0.588 to 0.627. The stopband corresponds to the peak in the reflectance spectrum of PS-RhB PhC, which is shown by the blue curve in Fig. 4(b). The peak's FWHM is slightly larger than the band gap, since the band diagram is calculated by assuming the PhC to be infinite and the reflectance spectrum is calculated for a sample of finite thickness. The comparison between the results of these independent calculations shows that the KKR method is quite efficient in predicting the wavelength and estimating the width of the photonic stopband. The reflectance spectrum for $\varepsilon = 2.5281 - 0.05i$ is plotted in Fig. 4(b) by the green curve. The reflectance of the PhC is seen to exceed unity (dotted line) between 0.555 and 0.638, as a result of emission. The reflectance is enhanced near the band edges of the PhC and suppressed at the center of the stopband (marked by the arrow). In ideal PhCs, the maximum enhancement in the reflection should be exactly at the band edges, due to the smallest group velocity of the propagating mode. This is not the case in real finite-size PhCs, since the wave vector component parallel to the propagation direction is not well defined. However, one may still expect the emission enhancement to occur near the band edges, at frequencies marked by the dashed lines in Fig. 4 [9].

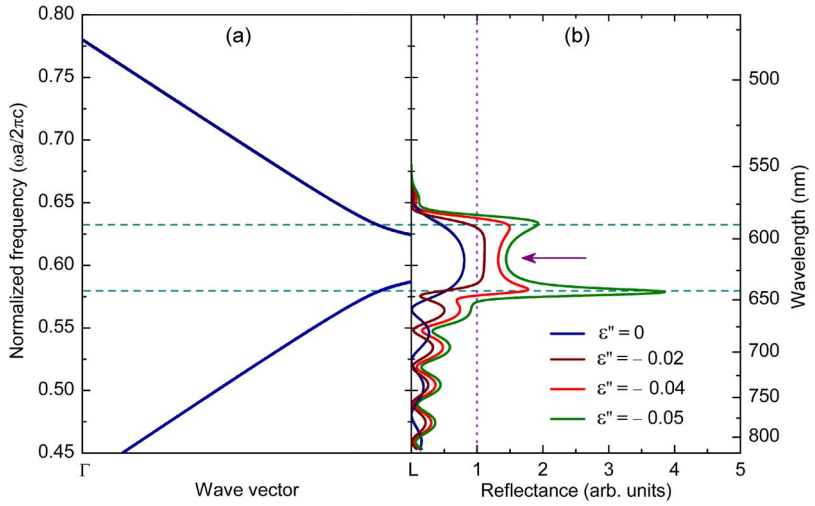

Fig. 4. (a) Dispersion of PS-RhB PhC along the ΓL direction and (b) the corresponding specular reflectance spectra calculated using KKR method for different ε''. Reflectance may exceed unity (dotted vertical line) due to the emission. Arrow shows maximum suppression of emission due to the photonic stopband.

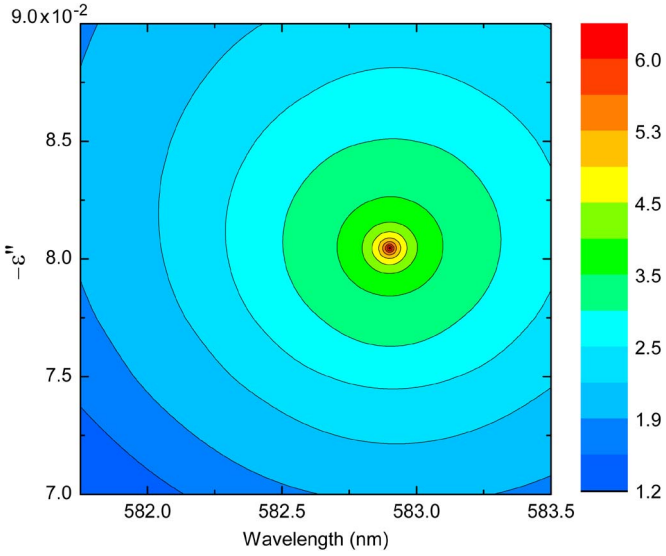

Fig. 5. Reflectance (in logarithmic scale) from PS-RhB PhC as a function of wavelength and ϵ''. The reflectance corresponds to the $L + 22^\circ$ direction and diverges at the wavelength near 582.7 nm and $\epsilon'' \approx -0.0802$.

After verifying the accuracy of the KKR method with the dispersion relation in the ΓL direction, we repeat the calculation for the $L + 22^\circ$ direction with the aim to estimate the lasing parameters. As it was mentioned earlier, the lasing corresponds to the divergency in the reflectance. Fig. 5 shows the contour plots of reflectance from PS-RhB PhC as a function of wavelength and ϵ'' in the vicinity of the low-wavelength edge of the PhC stopband. The logarithmic scale of reflectance is shown on the right side. One can see that the reflectance is divergent at the wavelength of about 583 nm, with the lasing threshold $\varepsilon''_{\text{th}} \approx -0.08$. The 4-nm difference between the experimental (587 nm) and theoretical values of the lasing wavelength can be explained by the size distribution of PS-RhB nanospheres, which was neglected in the theoretical analysis. The permittivity of PS-RhB colloids is related to the gain coefficient γ via [35] $|\varepsilon''|k_0 = \gamma\sqrt{\varepsilon'}$, where k_0 is the free space propagation

constant. This relation gives the threshold gain coefficient of 5436 cm^{-1}. Although this value is quite large, it may be reduced significantly (without a change in the lasing wavelength) by increasing the number of layers constituting the PhC.

As a concluding remark, we wish to iterate that the lasing from the PS-RhB PhC observed in our experiments occurs essentially due to the DFB enhancement near the stopband edge. The lasing wavelength is determined by the spectral positions of the stopband and photoluminescence band. Hence, the spectral tuning of lasing is possible via the adjustment of either the stopband or photoluminescence band.

5. Conclusion

We have studied room-temperature emission from an opal PhC in the vicinity of the photonic band edge. The PhC has been self-assembled from polystyrene nanospheres doped with RhB. It exhibits ASE for pump powers above 70 mW and starts featuring stimulated emission once the lasing threshold of 99 mW is achieved. We unambiguously demonstrated that the lasing occurs due to the enhancement in DFB resulting from the reduced group velocity near the blue edge of the photonic stopband. In order to study the lasing behavior of dye-activated PhCs theoretically, we have described the effect of light amplification using a complex-valued permittivity with a negative imaginary part. This simple approach enables one to estimate both the lasing wavelength and the minimal gain parameter required for lasing.

Acknowledgment

M. S. Reddy gratefully acknowledges Profs. S. Dhar and S. S. Major at the Department of Physics (IIT Bombay) for mentorship and providing the access to spectrophotometer.

References

[1] H. Benisty, V. Berger, J.-M. Gerard, D. Maystre, and A. Tchelnokov, *Photonic Crystals: Towards Nanoscale Photonic Devices*. New York, NY, USA: Springer-Verlag, 2005.

[2] E. Yablonovitch, "Inhibited spontaneous emission in solid-state physics and electronics," *Phys. Rev. Lett.*, vol. 58, no. 20, pp. 2059–2062, May 1987. [Online]. Available: http://link.aps.org/doi/10.1103/PhysRevLett.58.2059

[3] S. John, "Strong localization of photons in certain disordered dielectric superlattices," *Phys. Rev. Lett.*, vol. 58, no. 23, pp. 2486–2489, Jun. 1987. [Online]. Available: http://link.aps.org/doi/10.1103/PhysRevLett.58.2486

[4] Y. S. Zhou, X. H. Wang, B. Y. Gu, and F. H. Wang, "Switching control of spontaneous emission by polarized atoms in two-dimensional photonic crystals," *Phys. Rev. Lett.*, vol. 96, no. 10, pp. 103601-1–103601-4, Mar. 2006. [Online]. Available: http://link.aps.org/doi/10.1103/PhysRevLett.96.103601

[5] P. Lodahl, A. F. van Driel, I. S. Nikolaev, A. Irman, K. Overgaag, D. Vanmaekelbergh, and W. L. Vos, "Controlling the dynamics of spontaneous emission from quantum dots by photonic crystals," *Nature*, vol. 430, no. 7000, pp. 654–657, Aug. 2004. [Online]. Available: http://dx.doi.org/10.1038/nature02772

[6] M. Megens, J. E. G. J. Wijnhoven, A. Lagendijk, and W. L. Vos, "Fluorescence lifetimes and linewidths of dye in photonic crystals," *Phys. Rev. A*, vol. 59, no. 6, pp. 4727–4731, Jun. 1999. [Online]. Available: http://link.aps.org/doi/10.1103/PhysRevA.59.4727

[7] S. Y. Zhu, Y. Yang, H. Chen, H. Zheng, and M. S. Zubairy, "Spontaneous radiation and Lamb shift in three-dimensional photonic crystals," *Phys. Rev. Lett.*, vol. 84, no. 10, pp. 2136–2139, Mar. 2000. [Online]. Available: http://link.aps.org/doi/10.1103/PhysRevLett.84.2136

[8] S. John and T. Quang, "Spontaneous emission near the edge of a photonic band gap," *Phys. Rev. A*, vol. 50, no. 2, pp. 1764–1769, Aug. 1994. [Online]. Available: http://link.aps.org/doi/10.1103/PhysRevA.50.1764

[9] K. Sakoda, "Enhanced light amplification due to group-velocity anomaly peculiar to two- and three-dimensional photonic crystals," *Opt. Exp.*, vol. 4, no. 5, pp. 167–176, Mar. 1999. [Online]. Available: http://dx.doi.org/10.1364/OE.4.000167

[10] A. C. Scofield, S.-H. Kim, J. N. Shapiro, A. Lin, B. Liang, A. Scherer, and D. L. Huffaker, "Bottom–up photonic crystal lasers," *Nano Lett.*, vol. 11, no. 12, pp. 5387–5390, Nov. 2011. [Online]. Available: http://pubs.acs.org/doi/abs/10.1021/nl2030163

[11] D. Englund, H. Altug, B. Ellis, and J. Vuèkovi, "Ultrafast photonic crystal lasers," *Laser Photon. Rev.*, vol. 2, no. 4, pp. 264–274, Aug. 2008. [Online]. Available: http://dx.doi.org/10.1002/lpor.200710032

[12] X. Wu, A. Yamilov, X. Liu, S. Li, V. P. Dravid, R. P. H. Chang, and H. Cao, "Ultraviolet photonic crystal laser," *Appl. Phys. Lett.*, vol. 85, no. 17, pp. 3657–3659, Oct. 2004. [Online]. Available: http://dx.doi.org/10.1063/1.1808888

[13] O. Painter, R. K. Lee, A. Scherer, A. Yariv, J. D. O'Brien, P. D. Dapkus, and I. Kim, "Two-dimensional photonic band-gap defect mode laser," *Science*, vol. 284, no. 5421, pp. 1819–1821, Jun. 1999. [Online]. Available: http://www.sciencemag.org/content/284/5421/1819.full.pdf

[14] P.-H. Weng, T.-T. Wu, T.-C. Lu, and S.-C. Wang, "Threshold gain analysis in GaN-based photonic crystal surface emitting lasers," *Opt. Lett.*, vol. 36, no. 10, pp. 1908–1910, May 2011. [Online]. Available: http://ol.osa.org/abstract.cfm?URI=ol-36-10-1908
[15] J. P. Dowling, M. Scalora, M. J. Bloemer, and C. M. Bowden, "The photonic band edge laser: A new approach to gain enhancement," *J. Appl. Phys.*, vol. 75, no. 4, pp. 1896–1899, Feb. 1994. [Online]. Available: http://dx.doi.org/10.1063/1.356336
[16] L. Florescu, K. Busch, and S. John, "Semiclassical theory of lasing in photonic crystals," *J. Opt. Soc. Amer. B*, vol. 19, no. 9, pp. 2215–2223, Sep. 2002. [Online]. Available: http://www.opticsinfobase.org/josab/abstract.cfm?URI=josab-19-9-2215
[17] Y. Nishijima, K. Ueno, S. Juodkazis, V. Mizeikis, H. Misawa, M. Maeda, and M. Minaki, "Tunable single-mode photonic lasing from zirconia inverse opal photonic crystals," *Opt. Exp.*, vol. 16, no. 18, pp. 13676–13684, Sep 2008. [Online]. Available: http://dx.doi.org/10.1364/OE.16.013676
[18] L. K. Teh, C. C. Wong, H. Y. Yang, S. P. Lau, and S. F. Yu, "Lasing in electrodeposited ZnO inverse opal," *Appl. Phys. Lett.*, vol. 91, no. 16, pp. 161116-1–161116-1, Oct. 2007. [Online]. Available: http://dx.doi.org/10.1063/1.2801358
[19] M. N. Shkunov, Z. V. Vardeny, M. C. DeLong, R. C. Polson, A. A. Zakhidov, and R. H. Baughman, "Tunable, gap-state lasing in switchable directions for opal photonic crystals," *Adv. Funct. Mat.*, vol. 12, no. 1, pp. 21–26, Jan. 2002. [Online]. Available: http://eprints.soton.ac.uk/262523/
[20] K. Yoshino, S. Tatsuhara, Y. Kawagishi, M. Ozaki, A. A. Zakhidov, and Z. V. Vardeny, "Amplified spontaneous emission and lasing in conducting polymers and fluorescent dyes in opals as photonic crystals," *Appl. Phys. Lett.*, vol. 74, no. 18, pp. 2590–2592, May 1999. [Online]. Available: http://dx.doi.org/10.1063/1.123907
[21] S. Kedia, R. Vijaya, A. K. Ray, and S. Sinha, "Laser emission from self-assembled active photonic crystal matrix," *J. Nanophoton.*, vol. 4, no. 1, p. 049506, Oct. 2010. [Online]. Available: http://dx.doi.org/10.1117/1.3506524
[22] R. V. Nair and R. Vijaya, "Structural and optical characterization of photonic crystals synthesized using the inward growing self-assembling method," *Appl. Phys. A*, vol. 90, no. 3, pp. 559–563, Mar. 2008. [Online]. Available: http://dx.doi.org/10.1007/s00339-007-4326-9
[23] S. Johnson and J. Joannopoulos, "Block-iterative frequency-domain methods for Maxwell's equations in a planewave basis," *Opt. Exp.*, vol. 8, no. 3, pp. 173–190, Jan. 2001. [Online]. Available: http://www.opticsexpress.org/abstract.cfm?URI=oe-8-3-173
[24] Y. A. Vlasov, V. N. Astratov, A. V. Baryshev, A. A. Kaplyanskii, O. Z. Karimov, and M. F. Limonov, "Manifestation of intrinsic defects in optical properties of self-organized opal photonic crystals," *Phys. Rev. E*, vol. 61, no. 5, pp. 5784–5793, May 2000. [Online]. Available: http://link.aps.org/doi/10.1103/PhysRevE.61.5784
[25] L. Bechger, P. Lodahl, and W. L. Vos, "Directional fluorescence spectra of laser dye in opal and inverse opal photonic crystals," *J. Phys. Chem. B*, vol. 109, no. 20, pp. 9980–9988, Apr. 2005. [Online]. Available: http://pubs.acs.org/doi/abs/10.1021/jp047489t
[26] S. G. Romanov, M. Bardosova, D. E. Whitehead, I. M. Povey, M. Pemble, and C. M. Sotomayor Torres, "Erasing diffraction orders: Opal versus Langmuir–Blodgett colloidal crystals," *Appl. Phys. Lett.*, vol. 90, no. 13, pp. 133101-1–133101-3, Mar. 2007. [Online]. Available: http://dx.doi.org/10.1063/1.2714198
[27] J. F. Galisteo-Lopez, E. Palacios-Lidon, E. Castillo-Martinez, and C. Lopez, "Optical study of the pseudogap in thickness and orientation controlled artificial opals," *Phys. Rev. B*, vol. 68, no. 11, pp. 115109-1–115109-8, Sep. 2003. [Online]. Available: http://link.aps.org/doi/10.1103/PhysRevB.68.115109
[28] R. V. Nair and R. Vijaya, "Observation of higher-order diffraction features in self-assembled photonic crystals," *Phys. Rev. A*, vol. 76, no. 5, pp. 053805-1–053805-7, Nov. 2007. [Online]. Available: http://link.aps.org/doi/10.1103/PhysRevA.76.053805
[29] M. S. Reddy, R. Vijaya, I. D. Rukhlenko, and M. Premaratne, "Spatial and spectral distributions of emission from dye-doped photonic crystals in reflection and transmission geometries," *J. Nanophoton.*, vol. 6, no. 1, p. 063526, Nov. 2012. [Online]. Available: http://dx.doi.org/10.1117/1.JNP.6.063526
[30] M. Shkunov, M. DeLong, M. Raikh, Z. Vardeny, A. Zakhidov, and R. Baughman, "Photonic versus random lasing in opal single crystals," *Synth. Metals*, vol. 116, no. 1–3, pp. 485–491, Jan. 2001. [Online]. Available: http://www.sciencedirect.com/science/article/pii/S0379677900004203
[31] K. Sakoda, K. Ohtaka, and T. Ueta, "Low-threshold laser oscillation due to group-velocity anomaly peculiar to two- and three-dimensional photonic crystals," *Opt. Exp.*, vol. 4, no. 12, pp. 481–489, Jun. 1999. [Online]. Available: http://dx.doi.org/10.1364/OE.4.000481
[32] N. Stefanou, V. Yannopapas, and A. Modinos, "Heterostructures of photonic crystals: Frequency bands and transmission coefficients," *Comput. Phys. Commun.*, vol. 113, no. 1, pp. 49–77, Sep. 1998. [Online]. Available: http://dx.doi.org/10.1016/S0010-4655(98)00060-5
[33] N. Stefanou, V. Yannopapas, and A. Modinos, "MULTEM 2: A new version of the program for transmission and band-structure calculations of photonic crystals," *Comput. Phys. Commun.*, vol. 132, no. 1/2, pp. 189–196, Oct. 2000. [Online]. Available: http://dx.doi.org/10.1016/S0010-4655(00)00131-4
[34] A. Yariv, *Quantum Electronics*. New York, NY, USA: Wiley, 1967.
[35] D. Handapangoda, I. D. Rukhlenko, M. Premaratne, and C. Jagadish, "Optimization of gain-assisted waveguiding in metal-dielectric nanowires," *Opt. Lett.*, vol. 35, no. 24, pp. 4190–4192, Dec. 2010. [Online]. Available: http://dx.doi.org/10.1364/OL.35.004190